



Finite element analysis and modeling of structure with bolted joints

Jeong Kim ^{a,*}, Joo-Cheol Yoon ^b, Beom-Soo Kang ^c

^a Department of Aerospace Engineering, Pusan National University, ERC/NSDM, San 30, Jangjeon-Dong, Kumjeong-Ku, Busan 609-735, Republic of Korea

^b Research & Development Division, Hyundai Motor Company, Hwaseong 445-706, Republic of Korea

^c ERC/NSDM, Pusan National University, Busan 609-735, Republic of Korea

Received 1 October 2003; received in revised form 1 November 2005; accepted 30 March 2006

Abstract

In this work, in order to investigate a modeling technique of the structure with bolted joints, four kinds of finite element models are introduced; a solid bolt model, a coupled bolt model, a spider bolt model, and a no-bolt model. All the proposed models take into account pretension effect and contact behavior between flanges to be joined. Among these models, the solid bolt model, which is modeled by using 3D solid elements and surface-to-surface contact elements between head/nut and the flange interfaces, provides the best accurate responses compared with the experimental results. In addition, the coupled bolt model, which couples degree of freedom between the head/nut and the flange, shows the best effectiveness and usefulness in view of computational time and memory usage. Finally, the bolt model proposed in this study is adopted for a structural analysis of a large marine diesel engine consisting of several parts which are connected by long stay bolts.

© 2006 Elsevier Inc. All rights reserved.

Keywords: FEM; Pretension; Bolted joint; Contact element; Structural analysis; Marine diesel engine

1. Introduction

A bolted joint is employed to hold two or more parts together to form an assembly in a mechanical structure. Two primary characteristics in the bolted joint are a pretension and a mating part contact. Previous studies on the structure with a bolted joint are mostly dedicated to extraction of stiffness for the joint region and estimation of contact stress through a detailed model for a bolted joint using the FEM [1–5]. Yorgun et al. [6] investigated the behavior of a double channel beam-to-column connection subjected to in plane bending moment and shear based on tests and finite element software ANSYS. Maggi et al. [7] also demonstrated using the same software how variations of geometric characteristics in bolted end plate could change the connection

* Corresponding author. Tel.: +82 51 510 2477; fax: +82 51 513 3760.
E-mail address: greatkj@pusan.ac.kr (J. Kim).

behavior. Zhang and Poirier [8] developed a new analytical model of bolted joints and took into consideration the stiffness reduction associated with the residual force on the assembly, compression deformation caused by external force and dimensions changing due to member rotation. However, due to its limitation, the analytical model is not applicable to bolted assemblies when the members are of different geometry or when the external forces are not symmetric about the member interface.

As a consequence of the earlier works, it was noted that in order to accurately predict the physical behaviors of the structure with a bolted joint, a detailed three-dimensional bolt model is desirable, which fully includes the friction due to the contact on mating parts and pretension effect to tie. However, for a large complex structure such as a marine diesel engine, the detailed modeling of the bolted joint is difficult because of restriction of the problem size and computational cost to analyze the entire structure. Therefore, in this paper, in order to investigate a finite element modeling technique of the structure with bolted joints, four kinds of finite element models are introduced; a solid bolt model, a coupled bolt model, a spider bolt model, and a no-bolt model. All the proposed models take into account pretension effect and contact behavior between flanges to be joined. Through a comparison with a static experiment and a modal test, the validation of the bolt models proposed in this work is confirmed. Among these models, a solid bolt model, which is modeled by using three-dimensional brick elements and surface-to-surface contact elements between the head/nut and the flange interfaces, provides the best accurate responses compared with the experimental results. Additionally, the coupled bolt model, which couples the degree of freedom between the head/nut and the flange, shows the best effectiveness and usefulness in view of computational time and memory usage. Finally, the bolt model proposed in this paper is adopted for a structural analysis of a large marine diesel engine consisting of several parts that are connected by long stay bolts. All numerical simulations are carried out using implicit FEM software package ANSYS.

2. Mathematical procedure

The structure with bolted joints to be analyzed is discretized with a number of elements and then assembled at nodes. The elements of different type and shape with complex loads and boundary conditions can be used simultaneously using FEM. Consider an element of volume V bounded by a surface S with the traction vector $\bar{\mathbf{t}}$ prescribed on a part of the surface S_F . The finite element formulation is to begin with a variational principle related to total potential energy as follows:

$$\pi = \int_V \boldsymbol{\sigma}^T \boldsymbol{\varepsilon} dV - \int_{S_F} \mathbf{u}^T \bar{\mathbf{t}} dS = 0, \quad (1)$$

where $\boldsymbol{\sigma}$, $\boldsymbol{\varepsilon}$ and \mathbf{u} are stress, strain and displacement vector, respectively. The first order variation of the functional Eq. (1) can be written as

$$\delta\pi = \int_V \boldsymbol{\sigma}^T \delta\boldsymbol{\varepsilon} dV - \int_{S_F} \delta\mathbf{u}^T \bar{\mathbf{t}} dS = 0. \quad (2)$$

Using constitutive equation $\boldsymbol{\sigma} = \mathbf{D}\boldsymbol{\varepsilon}$ and strain–displacement relation $\boldsymbol{\varepsilon} = \mathbf{B}\mathbf{u}$, the Eq. (2) is derived as

$$\delta\mathbf{u}^T \left[\int_V \mathbf{B}^T \mathbf{D} \mathbf{B} dV \right] \mathbf{u} - \delta\mathbf{u}^T \int_{S_F} \mathbf{N} \bar{\mathbf{t}} dS = 0, \quad (3)$$

where \mathbf{N} is matrix of shape functions. Eq. (3) is the basic equation for the finite element discretization and can be converted to algebraic equations as follows:

$$\mathbf{K}\mathbf{u} = \mathbf{f}, \quad (4)$$

where \mathbf{K} is the element stiffness matrix, \mathbf{f} is the vector of surface loads. This equation system can be solved for unknown displacement vector \mathbf{u} using commercial FEM software. ANSYS used as an FEM code includes a full complement of nonlinear and linear elements, material laws ranging from metal to rubber, and the most comprehensive set of solvers available. It can handle even the most complex assemblies especially those involving nonlinear contact and is the ideal choice for determining stresses, temperatures, displacements and contact pressure distributions on all component and assembly designs. For contact problems, ANSYS can model con-

tact condition with contact element and present Lagrange multiplier, penalty function and direct constraint approach. When meshing a model, the nodes on potential contacting surfaces comprise the layer of contact elements whose four Gauss integral points are used as contacting checkpoints. ANSYS provides several element types to include surface-to-surface contact and frictional sliding. One of these elements is the 3D 8-node surface-to-surface contact element *CONTAC174*. ANSYS surface-to-surface contact elements use Gauss integration points as a default, which generally provides more accurate results than the Newton–Cotes/Lobatto nodal integration scheme, which uses the nodes themselves as the integration points [9]. The nodal detection algorithms also require the smoothing of the contact surface or the smoothing of the target surface, but which is quite time-consuming.

3. Finite element models for a bolted joint

In view of a finite element analysis, two primary characteristics of a bolted joint are a pretension and a mating part contact [10]. The pretension can generally be modeled with a thermal deformation, a constraint equation, or an initial strain. For a thermal deformation method, the pretension is generated by assigning virtual different temperatures and thermal expansion coefficients to the bolt and the flange. In the case of the constraint equation method, the pretension is a special form of coupling, with which equations can be applied to govern the behavior of the associated nodes. Initial strain method is more direct approach, in which the initial displacement is considered as a portion of the pretension on the structure with a bolted joint. A contact modeling can be addressed using point-to-point, point-to-surface, or surface-to-surface elements [11,12].

In this work, in order to generate a finite element model for the structure with a bolted joint, four kinds of bolt models are introduced. All the proposed models take into account above primary characteristics such as a pretension effect and a contact behavior between flanges.

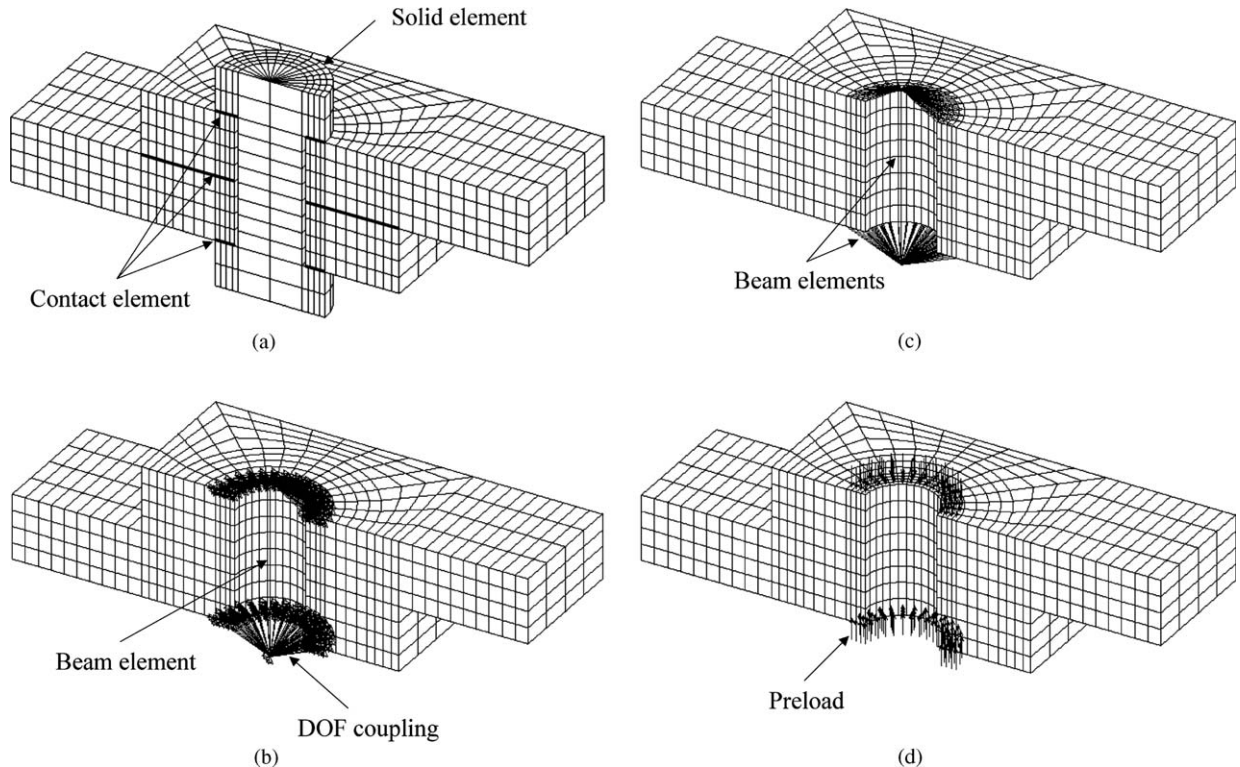


Fig. 1. Finite element models for the structure with a bolted joint. (a) Solid bolt model, (b) coupled bolt model, (c) spider bolt model and (d) no-bolt model.

3.1. Solid bolt model

The solid bolt model as shown in Fig. 1(a) is the most realistic finite element model among them, which is modeled by using three-dimensional brick elements, as called SOLID45 in ANSYS. The element is defined by eight nodes and each having three degrees of freedom. In addition, a surface-to-surface contact elements, which consists of contact elements (CONTAC174) and target segment elements (TARGE170), is used on the interfaces between the bolt head and the upper flange, the nut and the lower flange, and between the upper and lower flanges. In this bolt model, in order to apply clamping force over the bolt, virtual thermal deformation method is employed. In the method, the thermal expansion coefficient is assumed to be unit and the temperature difference ΔT is regarded as the following relation:

$$\Delta T = \frac{4P_0}{\pi d^2 E}, \quad (5)$$

where E is elastic modulus of the material, an effective diameter of the bolt d and the clamping force P_0 .

3.2. Coupled bolt model

In the coupled bolt model as shown in Fig. 1(b), it is much simpler than the solid bolt model. The stud of a bolt is approximately modeled by a beam element, and the nodes corresponding to the head and the nut are connected to the stud by means of the DOF coupling. The beam element, as called BEAM4 in ANSYS, is a uniaxial element with tension, compression, torsion, and bending capabilities. As a result of the coupling condition, its associated nodes are forced to take the same displacement in the specified nodal coordinate direction so that the structure with bolted joints can be influenced by the pretension effect. In this approach, since only beam element is used to represent the bolted joint, the number of finite elements is significantly reduced compared to the solid bolt model. The pretension effect can be considered by directly applying an initial strain ε_0 to the stud as the following:

$$\varepsilon_0 = \frac{4P_0}{\pi d^2 E}. \quad (6)$$

However, there are no contact elements between the bolt and the flanges in this bolt model.

3.3. Spider bolt model

The spider bolt model is composed of three-dimensional beam elements for all components, i.e. a stud, a head and a nut as shown in Fig. 1(c). Hence, in this bolt model, the stud is represented by beam elements in the same as the coupled bolt model, and both of the head and nut are also modeled with a series of beam elements in a web-like fashion. Since the head (or nut) and flange are connected with each other by beam elements, various loads can be transferred and the head (or nut) stiffness can be considered as well. But in the spider bolt model, physical properties of a beam element such as the cross-sectional area, the area moment of inertia, the height and so on have to be set to exactly assess the head and nut stiffness. To do this, the total volume of beam elements for the head (or nut) is assumed to be equal to that of the actual head (or nut) in this study.

3.4. No-bolt model

In this no-bolt model, there is no finite element model to directly describe the bolt components as shown in Fig. 1(d). The pressure corresponding to the clamping force is imposed on the washer surface to adopt the pretension effect. Hence, the no-bolt simulation is the easiest way among the bolt models proposed in this study. However, the no-bolt model cannot consider the influence of the bolt stiffness on simulation, and also cannot take into account the change of the bolt load due to application of a constant clamping force. It is noticed that this no-bolt model should be used in case it is not required to consider the bolt stiffness and no separation takes place between parts.

Except the solid bolt model, other three modeling techniques require a simplification procedure to create a finite element model from an actual bolted joint. Thus, it is recommended that one should firstly determine what bolt characteristic has to be considered based on precise understanding of the behavior of the bolted joint.

3.5. Mesh density

In order to confirm mesh density used in the above finite element models, case studies with different mesh sizes on the solid bolt models among four kinds of bolt models were carried out. The bolted joint connection used in the case studies is composed of two plates, which has a width of 40 mm, a thickness of 10 mm and a length of 60 mm individually and joined with an M10 bolt. Fig. 2 shows comparison of FE models created using different mesh sizes. The material of the bolt and the plate is assumed to be linear elastic behavior during clamping. The input mechanical properties of the material used in linear elastic FE analysis for the bolted joint connection are Young's modulus of 200 GPa and poisson's ratio of 0.3. The clamping force P_0 is 1500 N. Table 1 lists total number of nodes, elements and their corresponding computational CPU times run with each bolt model using an Alpha-433 machine. As listed in the table, finer mesh takes more elapsed CPU time for all

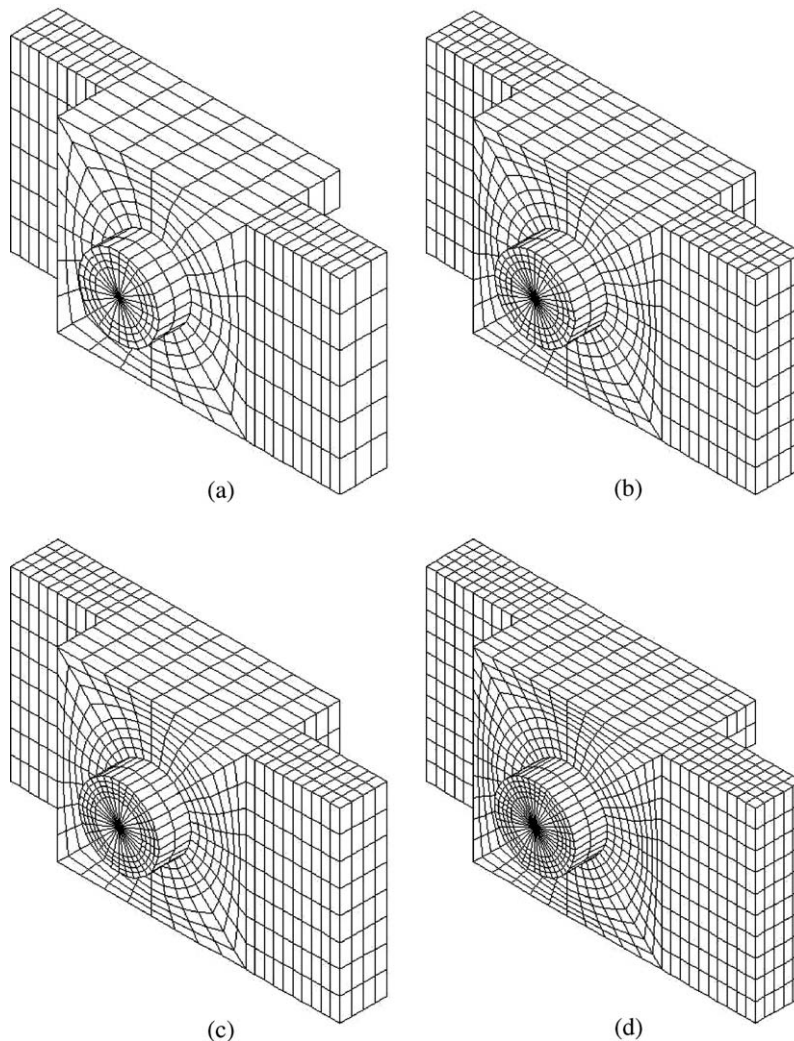


Fig. 2. Comparison of FE models using different mesh sizes. (a) Case A, (b) case B, (c) case C and (d) case D.

Table 1
Analysis cases for each bolt model

		Case A	Case B	Case C	Case D
Solid bolt Model	Elapsed CPU time [s]	55.150	107.507	163.785	363.700
	No. of nodes	3237	5745	6257	10013
	No. of elements	2952	5376	5888	9560
Coupled bolt Model	Elapsed CPU time [s]	37.167	84.827	100.686	233.197
	No. of nodes	2491	4751	5071	8531
	No. of elements	2098	4170	4490	7730
Spider bolt Model	Elapsed CPU time [s]	40.118	99.966	111.039	268.865
	No. of nodes	2491	4751	5071	8531
	No. of elements	2290	4490	4810	8210

bolt models. However, even with finer mesh, there is almost no variation of the displacements between Case C and D as shown in Fig. 3. Here, the displacements at the right end of the upper plate in the x and z directions are obtained from the FE simulation results. From the case studies, it is concluded that the mesh density of the Case C is adequate from the viewpoint of both efficiency and accuracy.

4. Verification of the finite element models for a bolted joint

4.1. Static experiment

In order to verify the four kinds of bolt models proposed in the previous chapter, comparison between the experiment and simulation results on the bolt models is carried out. The specimen used in the experiment is composed of two long plates, which has a width of 31.6 mm, a thickness of 8.46 mm and a length of 320 mm individually and joined with an M10 bolt [13]. Fig. 4 shows schematic view of the experimental setup and the positions of strain gauges. The experiment is simply executed by the deflection due to the static load of 10 N applied at the free end of a strip. Table 2 lists the measured x -direction strain components and the predicted ones obtained from finite element analyses with three different bolt models. As listed in the table, in the positions of B and C simulation results are in good agreement with the experiment. However, at the position A, which is the nearest distance from the bolted joint, the solid bolt model shows the most accurate result among them. Fig. 5 represents the distribution of the equivalent stress of the test specimen along the direction through strain gauges. As shown in the figure, even though the overall distributions of the stress are similar to each other, big discrepancies are observed in the region near the bolted joint. Thus, the solid bolt model is expected to be able to exactly predict the stress distribution due to consideration of the pretension effect and contact treatment, nevertheless, in order to evaluate the stress distribution in that region, comparison of the actual measured stress is required.

Through the comparison of the static experiment, the accuracy of the bolt models proposed in this work are somewhat confirmed. However, since the experiment refers very simple case in the structure with bolted joints it is difficult to verify the usefulness of the bolt models in the structure under various loading conditions. Hence, in the next section, an additional evaluation is carried out using more general loading conditions.

4.2. Additional evaluation using general loading conditions

In order to evaluate the reliability of the bolt models under general loading conditions, the finite element analyses with three different loading cases are carried out. The bolted structure used in the simulation is the same as the one employed in Section 3.5 so that the portion occupied by the bolt is raised to well represent the effect of a bolt. Fig. 6 shows three types of the loading conditions, i.e. two types of bending and a shear force. Fig. 7 displays the equivalent stress along the longitudinal direction of the plate from the center of the bolt with regard to different loading conditions. As mentioned previously, the simulation results far from the bolt center show little difference. On the other hand, Fig. 8 plots the stress distribution along the circum-

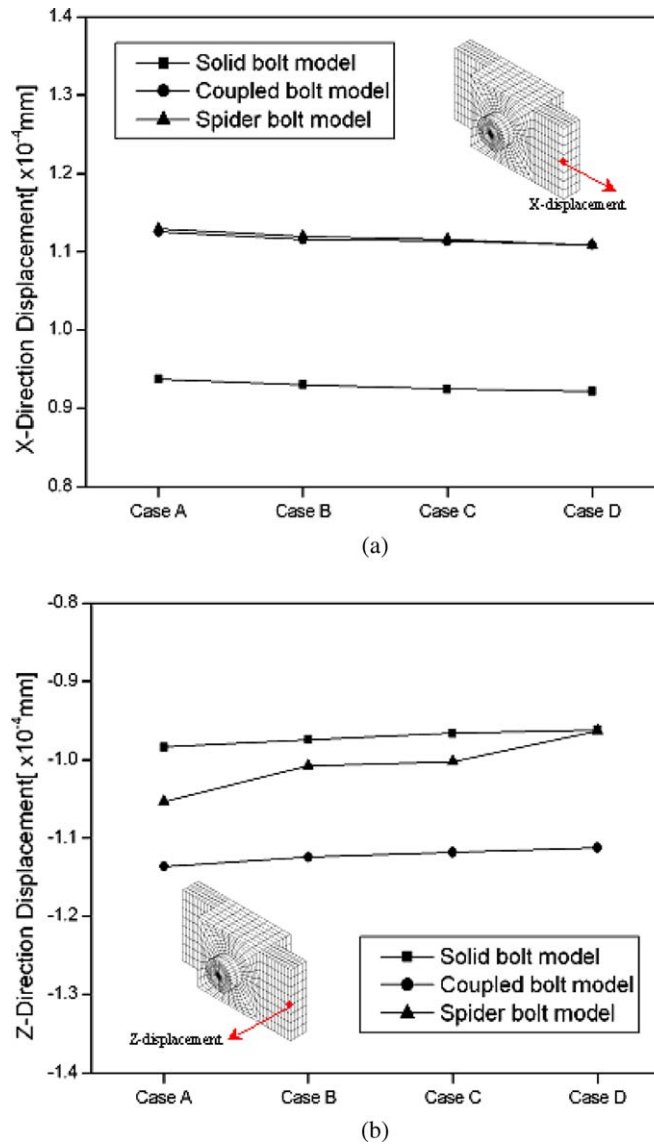


Fig. 3. Comparison of displacements obtained from FE simulation using different mesh sizes. (a) Displacements in the x -direction and (b) displacements in the z -direction.

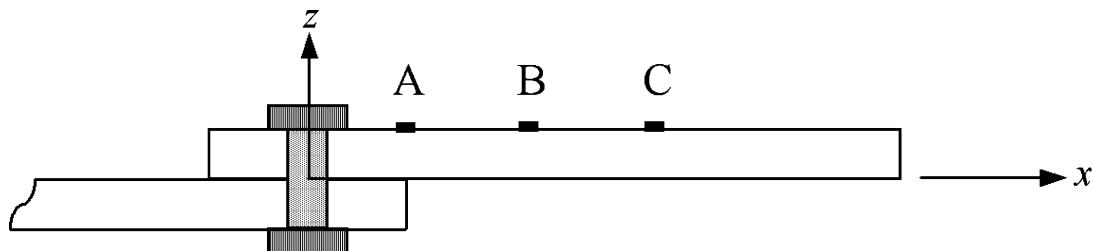


Fig. 4. Positions of strain gauges for static experiment.

ferential direction at a distance of a bolt radius from the bolt center on the interface surface between two plates. As shown in the figure, the simulation results near the bolted joint are dissimilar to each other due to

Table 2
Strains obtained from the experiment and finite element analysis [$\times 10^{-5}$]

Position	A	B	C
Experiment	3.293	2.918	2.333
Solid bolt model	3.307	2.911	2.335
Coupled bolt model	3.478	2.910	2.335
Spider bolt model	2.989	2.910	2.335
No-bolt model	3.390	2.912	2.335

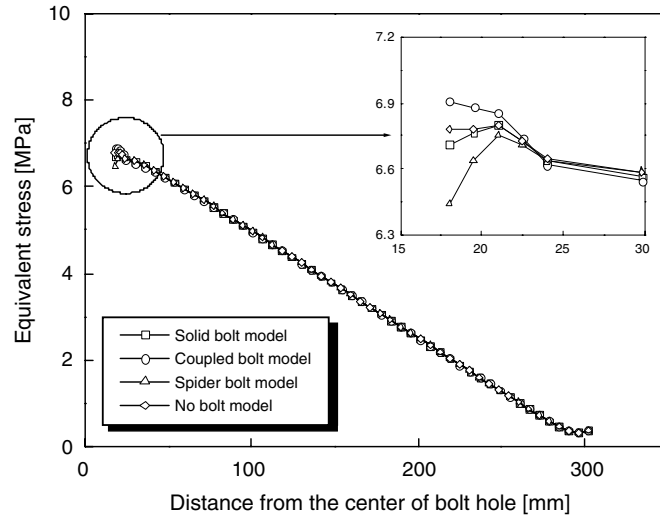


Fig. 5. Variation of the equivalent stress for each bolt model.

simplification of the bolt head and nut. In the case of bending, due to the deformation of the bolt head and nut, the locally different stress values are expected as shown in Fig. 8(a) and (b). Furthermore, in the case of shear loading, the distinction is remarkable as plotted in Fig. 8(c). It is because the friction force mostly maintains the structure on that occasion, thus the analysis result is largely dependent on how much the friction can be accurately considered. Fig. 9 shows the deformation configurations for each model under the bending as shown in Fig. 6(a). From the results, it is noted that the overall deformation modes are nearly the same each other.

The required memory size and computational time using an Alpha-433 machine for each model are listed in Table 3. As listed in the table, the coupled bolt model needs the minimum memory usage and computational cost, while the solid bolt model requires relatively large memory and computational time. The solid bolt model among the finite element models discussed here is recommended to predict the physical behaviors of the structure with a bolted joint accurately. However, in view of effectiveness and usefulness, the coupled bolt model might be also recommended.

4.3. Modal test

In order to confirm the utilization of the bolt models proposed in this study for a dynamic analysis, a series of modal analyses using the FEM are carried out and the comparison of the modal test results in Ref. [13] is made. The specimen used in the modal test is made of two plates joined with an M10 bolt, whose size is width of 31.6 mm, thickness of 8.46 mm and length of 320 mm. Fig. 10 shows the experimental setup for the modal test. By contrast with a static analysis, since the nonlinear features such as material nonlinearity, geometric nonlinearity, contact elements and so on, cannot be counted in a modal analysis, it is required to modify the bolt models previously used in the static analysis. Thus, the contact elements

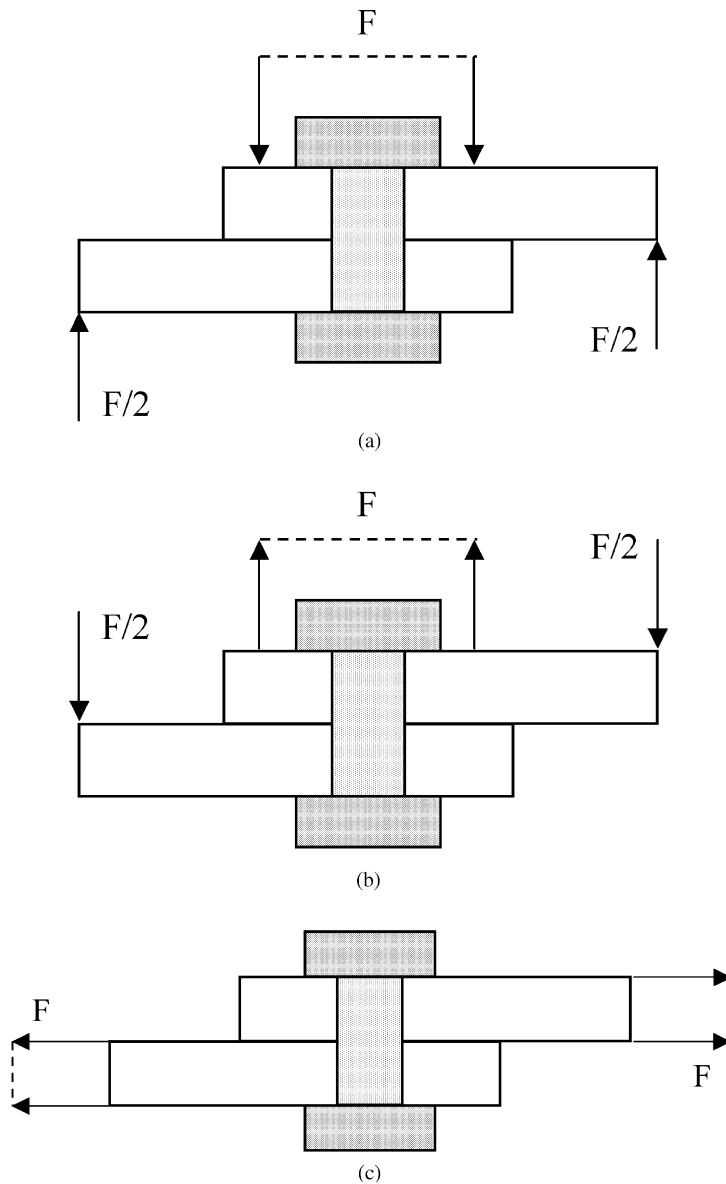
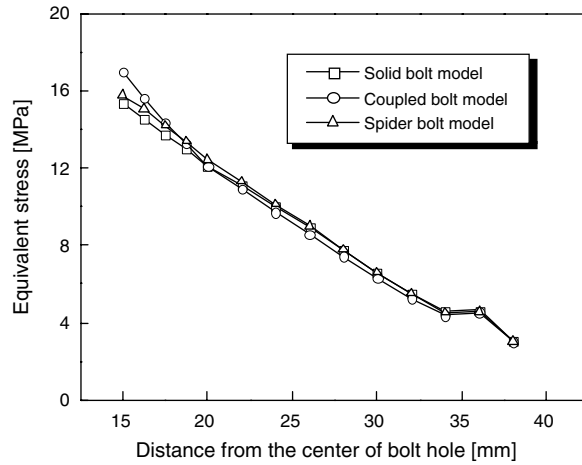


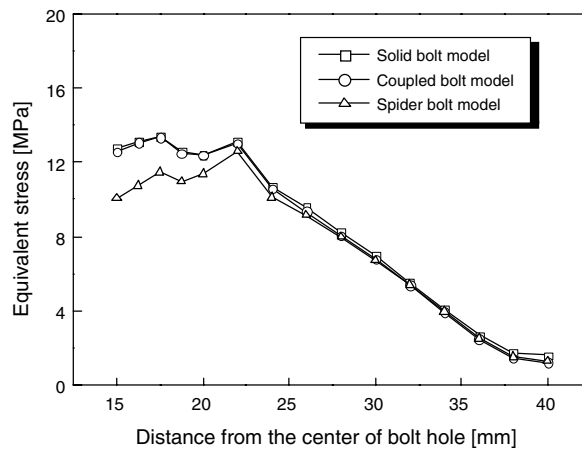
Fig. 6. Load conditions. (a) Bending type I, (b) bending type II and (c) Shearing.

created between two plates are deleted and then the region, where the stresses due to the clamping force are predominant, is glued each other. That region looks like a conical shape and covers a range between 25° and 33° suggested by Osgood [14], as shown in Fig. 11. The bolt head and the nut are also assumed to be adhered to the plates respectively due to the clamping force. Hence, in the case of the solid bolt model, the contact elements used on an interface surface are eliminated, and the bolt head and the nut become one united body along with the plates.

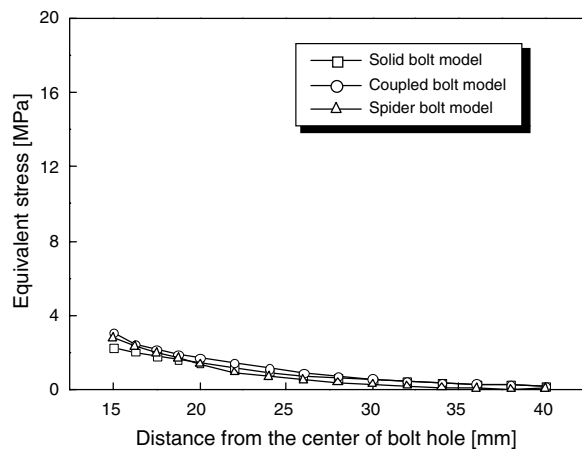
Table 4 lists the natural frequencies obtained from the modal test and the modal analysis using the FEM. As listed in the table, the experiment and simulation results are similar to each other. Fig. 12 shows several natural modes obtained from the modal analysis. Through a comparison of natural frequencies obtained from the modal analysis and test, it is concluded that the bolt models proposed in this study can be employed in a dynamic analysis as well as a static analysis.



(a)



(b)



(c)

Fig. 7. Variation of the equivalent stress with different loading conditions. (a) Under bending type I, (b) under bending type II and (c) under shearing.

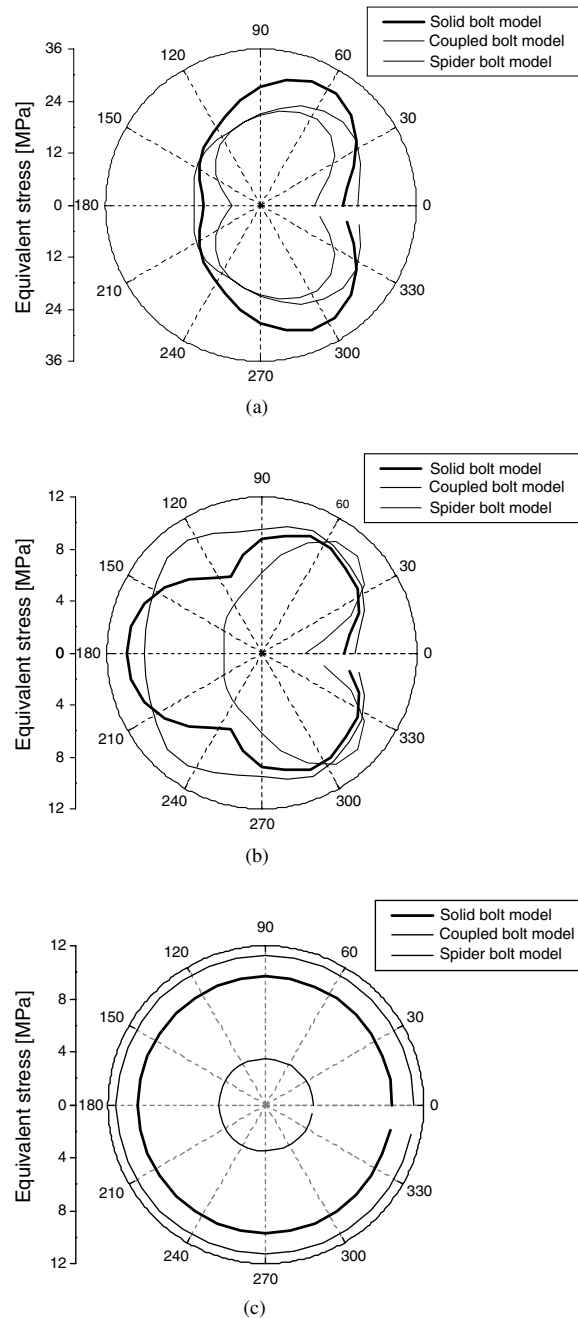


Fig. 8. Variation of the equivalent stress near the bolt head. (a) Under bending type I, (b) under bending type II and (c) under shearing.

5. Application to a large marine diesel engine

Low speed diesel engines are used for the propulsion for large ships such as a container ship, a bulk ship, as well as oil carriers, very large crude oil carrier (VLCC) and ultra large crude oil carrier (ULCC) because of its relatively high efficiency, power concentration and reliability [15]. In general, a large marine diesel engine is composed of a bed plate, a cylinder frame, a frame box and cylinder head components, which are joined each other with long stay bolts and thus become one large vertical structure as a single body. Since the engine

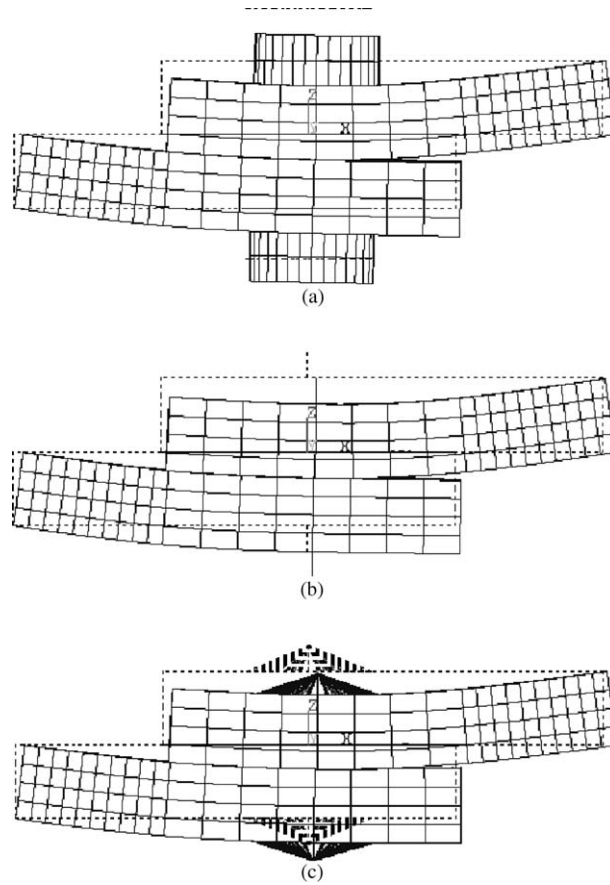


Fig. 9. Deformation shapes for each bolt model under bending. (a) Using solid bolt model, (b) using coupled bolt model and (c) using spider bolt model.

Table 3
Model usage and computational time for each bolt model

	Solid bolt model	Coupled bolt model	Spider bolt model
Model usage [MB]	10.69	8.34	8.56
Elapsed CPU time [s]	2843	1068	1446

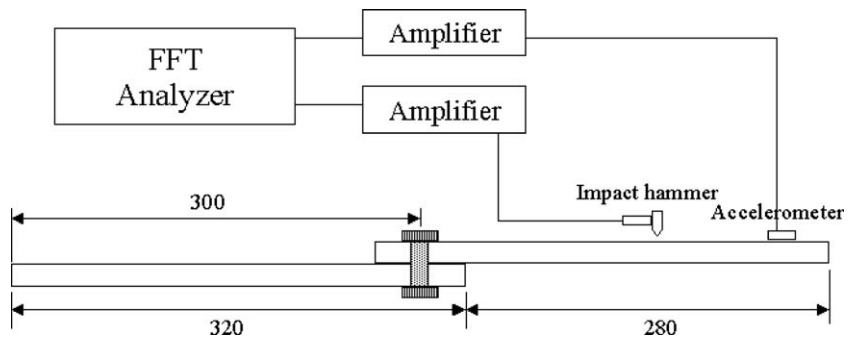


Fig. 10. Experimental setup for modal test (unit: mm).

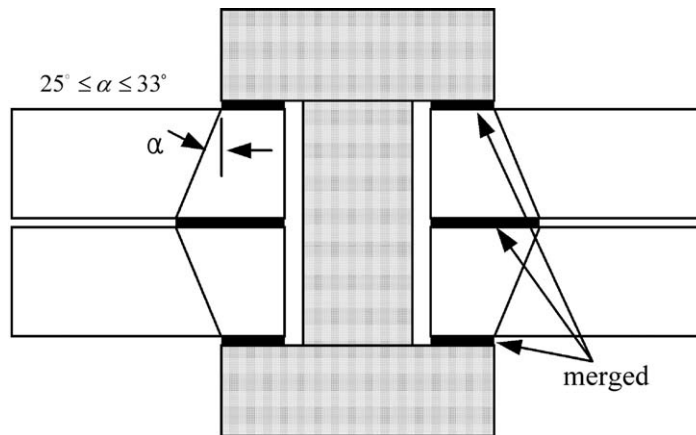


Fig. 11. Modified finite element model for modal analysis.

Table 4

Natural frequencies obtained from modal test and finite element analysis [unit: Hz]

Mode no.	1	2	3	4	5
Experiment	120.0	332.0	424.0	640.0	1060.0
Solid bolt model	119.4	334.0	426.5	634.9	1067.7
Coupled bolt model	121.0	334.3	431.9	643.4	1069.5
Spider bolt model	119.0	334.1	425.1	632.5	1068.0
No-bolt model	112.8	333.9	413.4	603.1	1068.0

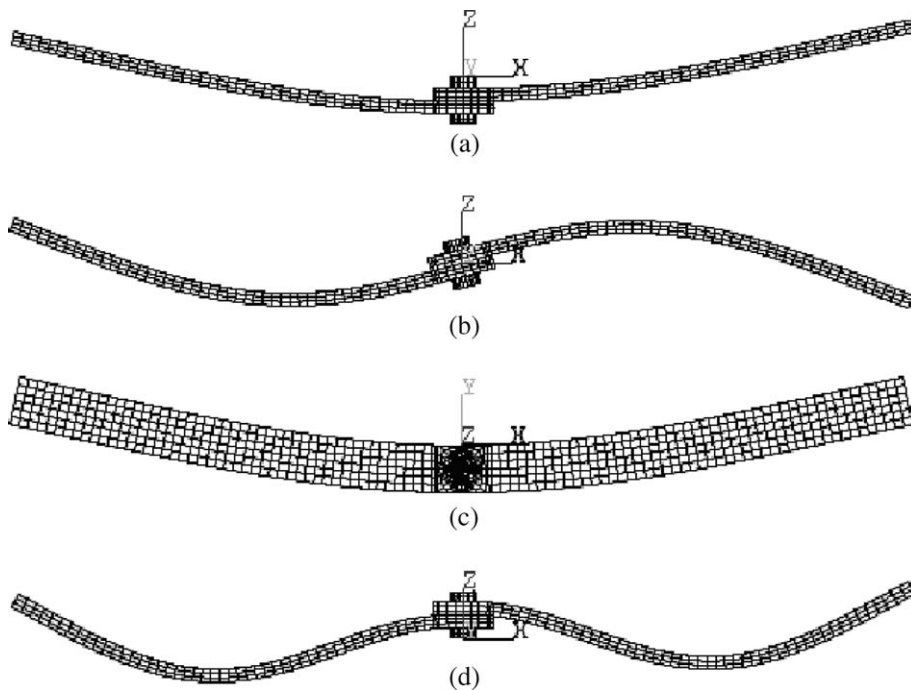


Fig. 12. Mode shapes of the specimen using a solid bolt model. (a) First mode at 119.4 Hz, (b) 2nd mode at 334.0 Hz, (c) 3rd mode at 426.5 Hz and (d) 4th mode at 634.9 Hz.

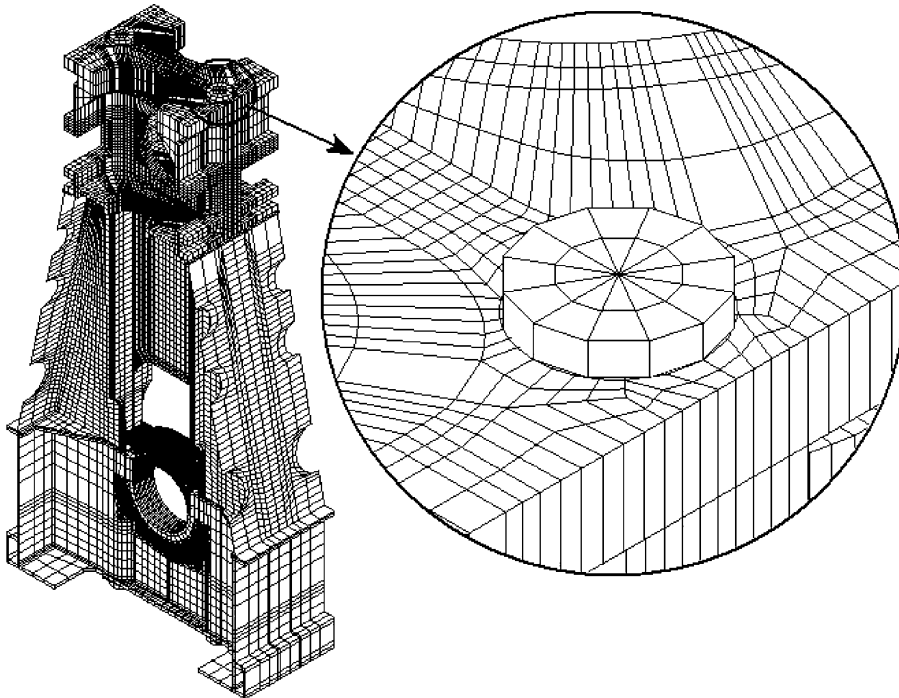


Fig. 13. Finite element model of an intermediate section between the cylinders 3–4.

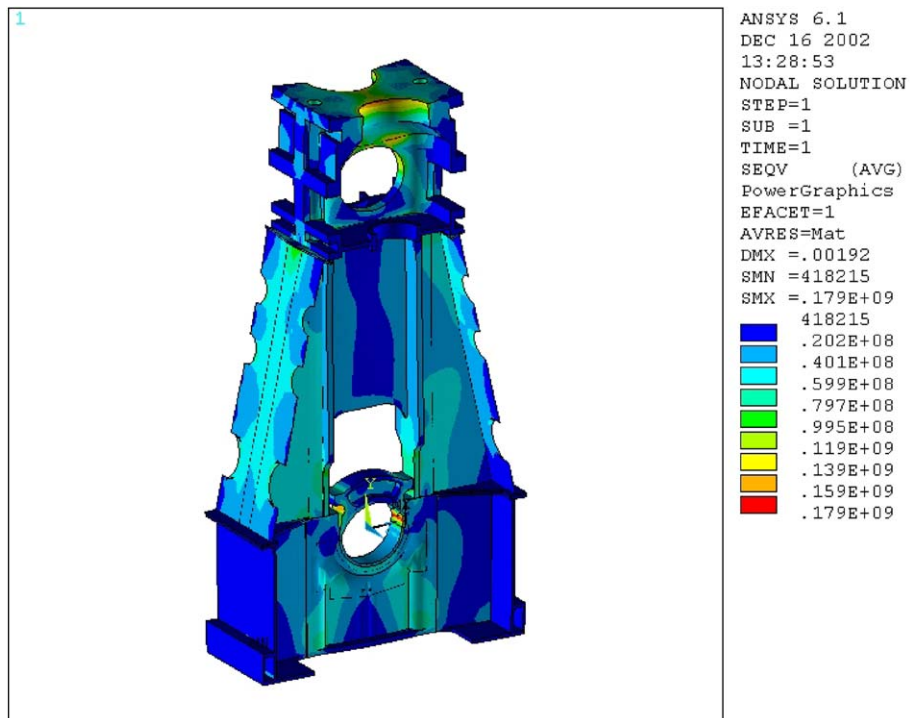


Fig. 14. Distribution of equivalent stress for the large marine diesel engine.

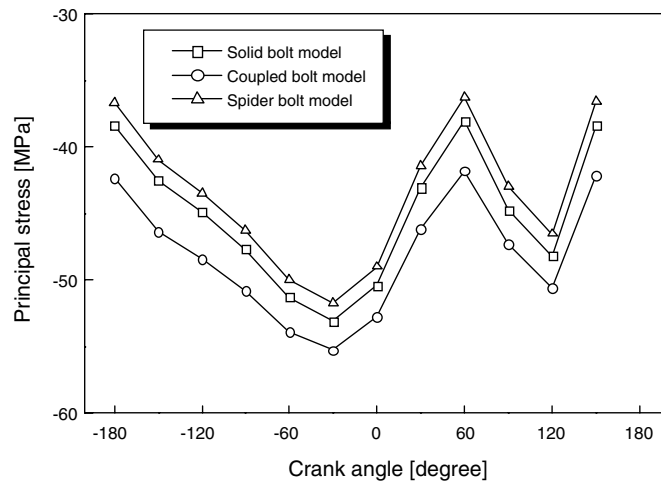


Fig. 15. Variation of the principal stresses near the bolted joint during one cycle.

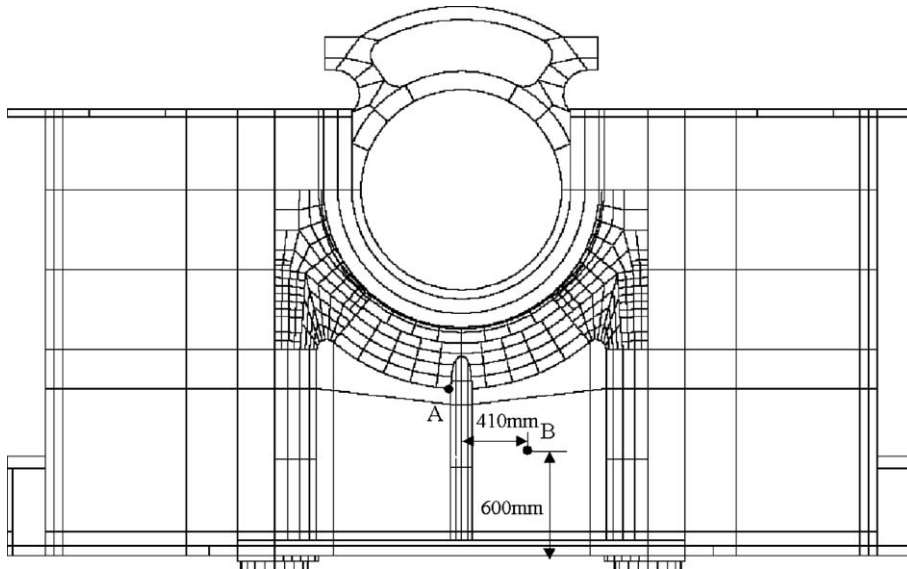
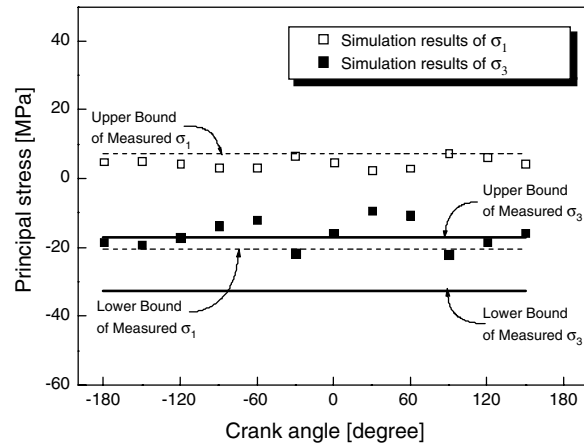


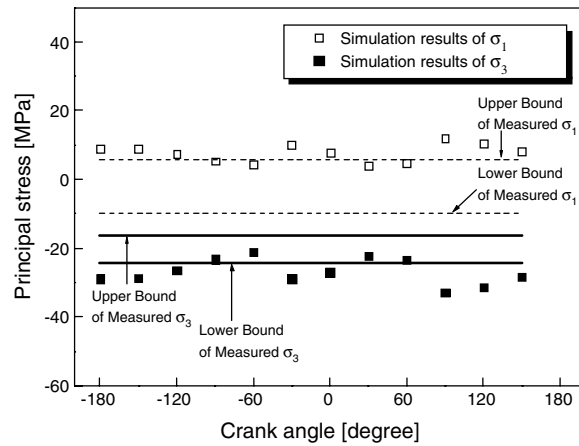
Fig. 16. Positions of measurement data.

structure employed in this study has 2-stroke 12 cylinders with the total output of more than 50 000 kW power, an one-twelfth symmetric model structure is considered. In order to predict the stress distribution for the diesel engine a three-dimensional finite element model is adopted as shown in Fig. 13. As mentioned previously, the engine structure used in the simulation is assembled via long stay bolts which combine and tighten each part by preventing separating. Moreover, since the clamping forces of the stay bolts are remarkably large compared to other loads, those forces affect extensively on distribution of the stress and the deformation of the overall engine structure. Hence, in order to more accurately estimate the effect of the stay bolts, the solid bolt model among the four kinds of bolt models is introduced in this application. In the solid bolt model, the stay bolt is modeled by an 8-node brick element, and contact elements are added on the interfaces between a head and a nut of the bolt.

Fig. 14 shows distribution of the equivalent stress for the simulated large marine diesel engine. From the results, it is found that the maximum stress occurs at the clamped region with stay bolts such as lower part



(a) At measure position A



(b) At measure position B

Fig. 17. Comparisons of the principal stresses obtained from finite element analyses and experiments. (a) At measure position A and (b) at measure position B.

of the bed plate. Fig. 15 illustrates variation of the principal stresses in the vicinity of the bolted joint during one cycle of the engine for each bolt model. As can be seen in the figure, there are no big differences according to each bolt model. Fig. 17 compares the principal stresses obtained from finite element analyses using a solid bolt model and experiments. Experimental data come from the upper and lower bound of the principal stresses measured at the positions A and B in Fig. 16 during one cycle of the engine. From the comparison between the simulation result and the measured one, it is well shown that the numerical model can predict stress distribution within the limit bounds. Consequently, the modeling technique using the bolt models proposed in this paper can give reasonable results to predict the structural behavior of a structure with bolted joints such as a large marine diesel engine.

6. Conclusions

In this paper, four kinds of the bolt models were suggested as a finite element modeling technique for the structure with a bolted joint. In addition, through a comparison with simple static experiment and modal test results, the effectiveness and usefulness of the bolt models were confirmed. The conclusions are summarized as the followings.

- (1) In order to generate a finite element model for the structure with a bolted joint, a solid bolt model, coupled bolt model, spider bolt model, and no-bolt model were suggested. Among them, the solid bolt model could most accurately predict the physical behavior of the structure.
- (2) In the case of shear loading, since the contact characteristic between interfaces is predominant, distinction with a difference in stress distribution, especially neighboring the bolted joint, is expected according to the bolt models.
- (3) From the result of static analysis, the coupled bolt model and the spider bolt model can save 62% and 49% of the computational time, and 21% and 19% of the memory usage compared to the solid bolt model. Therefore, in view of effectiveness and usefulness, the coupled bolt model is also recommended.

Acknowledgements

This work has been completed by the support of Brain Busan 21 Project, and the authors thank for this support. The last author's thank is extended to Professor S.H. Seong of School of Mechanical Engineering for providing the experimental data of a marine diesel engine.

References

- [1] H.H. Gould, B.B. Mikic, Areas of contact and pressure distribution in bolted joints, *Trans. ASME J. Mech. Des.* 94 (1972) 864–870.
- [2] J. Wileman, M. Choudhury, I. Green, Computation of member stiffness in bolted connections, *Trans. ASME J. Mech. Des.* 113 (1991) 432–437.
- [3] M. Nabil, Determination of joint stiffness in bolted connections, *Trans. ASME J. Mech. Des.* 98 (1976) 858–861.
- [4] J.H. Bickford, *An Introduction to the Design and Behavior of Bolted Joints*, 2nd ed., Marcel Dekker, 1990.
- [5] K. Schiffner, C.D. Helling, Simulation of prestressed screw joints in complex structures, *Comput. Struct.* 64 (1997) 995–1003.
- [6] C. Yorgun, S. Dalci, G.A. Altay, Finite element modeling of bolted steel connections designed by double channel, *Comput. Struct.* 82 (2004) 2563–2571.
- [7] Y.I. Maggi, R.M. Conclves, R.T. Leon, L.F.L. Ribeiro, Parametric analysis of steel bolted end plate connections using finite element modeling, *J Construct. Steel Res.* 61 (2005) 689–708.
- [8] O. Zhang, J. Poirier, New analytical model of bolted joints, *ASME J. Mech. Des.* 126 (2004) 721–728.
- [9] ANSYS Release 9.0 Documentation. ANSYS, Inc. Theory Reference.: ANSYS Inc., 2004.
- [10] J. Montgomery, Methods for modeling bolts in the bolted joint. ANSYS User's Conference 2002.
- [11] A.M. Habraken, S. Cescotto, Contact between deformable solids: the fully coupled approach, *Math. Comput. Model* 28 (1998) 153–169.
- [12] ANSYS Release 9.0 Documentation. Contact Technology Guide: ANSYS Inc., 2004.
- [13] Y.D. Kwon, N.S. Goo, S.Y. Kim, M.H. Cho, Finite element modeling for static and dynamic analysis of structures with bolted joints, *Trans. KSME A* 26 (2002) 667–676 (in Korean).
- [14] J.E. Shigley, *Mechanical Engineering Design*, McGraw-Hill, 1986.
- [15] J.R. Cho, B.Y. Lee, J.H. Kim, Structural analysis of low speed large diesel engine structures using CAD/CAE, *J. KSME* 21 (1997) 13–25 (in Korean).